An Improved Transient Model of Tool Temperatures in Metal Cutting

Tien-Chien Jen
Mechanical Engineering Department,
University of Wisconsin, Milwaukee,
Milwaukee, WI 53201

Aloysius U. Anagonye
Research & Development Center,
General Motors Corporation,
Warren, MI 49090

A model for predicting cutting tool temperatures under transient conditions is presented. The model of Stephenson et al. [10] is extended to include the initial transient response to the tool temperature and nonuniform heat flux distributions. The main goal in this paper is to be able to accurately predict the initial transient tool temperature response, or temperatures in interrupted cutting for cases where the cutting time is short. A method to predict the true transient energy partitioning instead of quasi-steady energy partitioning (Stephenson et al., [10]), without seeking the full numerical analysis, has been developed. In this paper, the transient energy partitioning is obtained through a fixed-point iteration process by modifying the quasi-steady energy partitioning method presented by Loewen and Shaw [11]. The predicted transient tool temperatures are compared quantitatively to the experimental data. Utilizing a semi-empirical correlation for heat flux distribution along the tool-chip interface, the temperature distribution is calculated and compared qualitatively to existing experimental data. [DOI: 10.1115/1.1334865]

Introduction

In machining operations, mechanical work is converted to heat through plastic deformation in chip formation and through friction between the tool and workpiece. Some of this heat conducts into the cutting tool, resulting in high tool temperatures near the cutting edge. Elevated tool temperatures have a negative impact on tool life. The tool becomes softer and wears more rapidly by abrasion as the temperature is increased. In many cases, constituents of the tool may diffuse into the chip or react chemically with the workpiece or cutting fluid.

Because of the impact on tool life, cutting temperatures have been widely studied. Most published research is restricted to steady-state temperatures in relatively simple processes. Examples are orthogonal cutting or cylindrical turning where the cutting speed, feed rate, and the depth of the cut are constant [1–7]. These restrictions hamper the accurate modeling of most industrial machining processes where these parameters vary with time and a steady-state temperature field is never established.

Recently, transient cutting temperatures have been investigated for interrupted turning, a process where the cutting speed, depth of cut, and feed rate remain constant, but the tool repeatedly enters and exits the workpiece, so that the heat input to the tool is periodic. Assuming the tool to be semi-infinite in all directions (i.e., a corner), Stephenson and Ali [8] used a Green's function approach to calculate tool temperatures in interrupted cutting. Their results agreed reasonably well with experimental data. Although the semi-infinite in all directions assumption may be adequate for interrupted cutting, where the heating times are on the order of 10 ms, it is likely not adequate for contour turning, where heating times are typically between 10 to 60 seconds. Furthermore, for cases where the heating time is short in comparison to the cooling time, the results of Stephenson and Ali [8] significantly underpredict the temperatures in the cutting zone. Radulescu and Kapoor [9] used the separation of variables method to solve the same problem for a finite tool, determining the temperature distributions in the workpiece and chip. They defined a chip formation zone (CFZ) in which heat is generated, and solved for the temperature distribution in the workpiece, the CFZ and the tool. Their results agreed well with experimental findings. Stephenson et al. [10] developed an improved model to account for the effects of the finite tool with transient heating for contour turning. They successfully eliminated the need to specify the convection boundary conditions at the ''exterior'' boundaries, as in Radulescu and Kapoor [9], and the semi-infinite domain assumption as in Stephenson and Ali [8]. With simplified ''interior'' boundary conditions, the temperature distribution at the tool-chip interface was calculated for two limiting boundary conditions, namely, isothermal and insulated thermal boundary conditions. Although results from these two cases bounded the experimental data, no improvements were reported in the short transient cases (as in Stephenson and Ali, [8]) in their study.

An improved model for predicting cutting tool temperatures under transient conditions is presented in this study. Recall that the energy partitioning method used in Stephenson and Ali [8] and Stephenson et al. [10] is valid *only* for quasi-steady conditions [11]. Loewen and Shaw used average temperature matching at the tool-chip interface to find the corresponding energy partitioning. At the chip side, the interface temperature is calculated by using the moving heat sources theory [12]. Although it has been shown [8,13] that the steady state temperature distribution can be established in a very short time, in many applications, such as milling and interrupted turning, the temperature at each cut-in may not reach steady state. Thus, steady-state energy partitioning methods result in underprediction of tool temperature in comparison to the initial transient energy partitioning method [14]. Temperature matching should still be valid even under the transient state so the task that remains is to estimate the transient temperature matching, and the corresponding transient energy partitioning. With a slight modification to Loewen and Shaw's model [11], the initial transient energy partitioning at the tool-chip interface can be obtained. It will be demonstrated that the initial energy partitioning is indeed much larger than the steady-state energy partitioning. The effect of variable heat flux distribution is studied. Comparisons to existing theoretical and experimental data are presented.

Theoretical Analysis

Tool Temperatures Model. Consider a cutting tool with a rectangular tool insert, cutting into the workpiece (Fig. 1). There is a heat source in the corner of one face of the tool insert, where it is in contact with the chip. To solve for the tool temperature distribution, a computational domain must be selected, and appro-

Contributed by the Manufacturing Engineering Division for publication in the JOURNAL OF MANUFACTURING SCIENCE AND ENGINEERING. Manuscript received January 1999; revised April 2000. Associate Editor: S. G. Kapoor.

priate boundary conditions specified. As the cutting progresses, the heat from the tool-chip interface penetrates further into the tool. Ideally, the computational domain should be chosen to be larger than the depth to which there is significant heat penetration. However, this depth is not known *a priori*. Furthermore, if the computational domain is chosen to be larger than the tool insert, then the thermal contact resistance at the tool-holder interface must be known in order to completely specify the problem. Unfortunately, typically this thermal contact resistance is not known to any precision, being dependent on the surface roughness of the interfaces and the contact pressure. The approach used in Stephenson et al. [10] is adopted here: the computational domain is chosen to be the same size as the tool insert, with approximate boundary conditions specified at the tool-holder interface. For this study, isothermal and insulated boundary conditions cases are studied. These boundary conditions are further discussed below.

The tool insert has three ''interior boundaries'' [10] in contact with the tool holder (at $x=0$, $y=e$, and $z=0$). Using the approach of Stephenson et al. [10], at the bottom surface of the insert ($y=e$, see Fig. 1), two types of thermal boundary conditions were considered to bound the actual situation: (a) ambient temperature, and (b) insulated surface. It is expected that the insulated boundary condition will yield a higher calculated temperature than the ambient temperature boundary condition. It was demonstrated in Stephenson et al. [10] that the actual (measured) temperature falls between the temperatures calculated for these two cases, being closer to the ambient temperature case than the insulated case. For the other two interior boundaries (these are farther from the heat source), only the ambient temperature boundary condition was used.

The other three ''exterior'' boundaries of the tool insert (at $x=d$, $y=0$, and $z=f$) are exposed to the environment (except where the tool is in contact with the chip). In most production processes, a water-based coolant is used to lubricate and to remove heat from the cutting zone. It was shown in Jen and Lavine [13] that the convection effect is very significant when a water-based cutting fluid is used. It was also shown that the convection effect is relatively insignificant if no coolant is used. In this paper, we only simulate the cases without coolant.

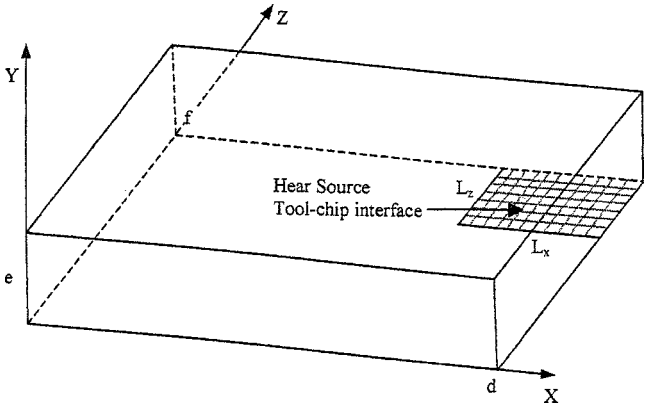

Fig. 1 Computational domain

With the above information, the problem can now be solved. The three-dimensional, transient heat conduction equation, assuming constant thermal properties, is:

$$\frac{1}{\alpha_T}\frac{\partial T}{\partial t}=\frac{\partial^2 T}{\partial x^2}+\frac{\partial^2 T}{\partial y^2}+\frac{\partial^2 T}{\partial z^2}+\frac{q(x,y,z,t)}{k_T} \tag{1}$$

where k_T and α_T are the tool thermal conductivity and thermal diffusivity, respectively. The source term, $q(x,y,z,t)$, can vary with time and position on the surface of the insert (see Stephenson and Ali [8] for possible heat flux distributions). Following the analysis of Chao and Trigger [15], Levy et al. [16] and Tsai [17], a parabolic heat flux distribution is assumed, and can be expressed as

$$q=\begin{cases} q_c''(a(t)x^2+b(t)x+c(t))\times\delta(y) & \ldots\ d-L_x\leqslant x\leqslant d;\quad f-L_z\leqslant z\leqslant L_z \\ 0 & \text{otherwise} \end{cases} \tag{2}$$

Here, $\delta(y)$ is the Dirac delta function and $q_c''(a(t)x^2+b(t)x+c(t))$ is the heat flux (as a function of x and t) entering the tool through the tool-chip interface (i.e., darkened region in Fig. 1) in the corner of the one surface (assumed rectangular even though it is not in reality). The coefficients $a(t)$, $b(t)$, and $c(t)$ are determined empirically from Levy et al. [16] and Kagiwada and Kanauchi [14]. A detailed discussion will be presented later. These coefficients can be expressed as follows:

$$a(t)=\begin{cases} a_0+a_s t & 0\leqslant t\leqslant t_s \\ \cdots\ \cdots & \\ a_s & t\geqslant t_s \end{cases}$$

$$b(t)=\begin{cases} b_0+b_s t & 0\leqslant t\leqslant t_s \\ \cdots\ \cdots & \\ b_s & t\geqslant t_s \end{cases} \tag{3}$$

$$c(t)=\begin{cases} b_0+b_s t & 0\leqslant t\leqslant t_s \\ \cdots\ \cdots & \\ b_s & t\geqslant t_s \end{cases}$$

Where

$$a_0=\frac{0.8-3R_2}{0.55L_x^2},\quad b_0=\frac{0.19+1.35R_2}{0.825L_x},\quad c_0=0.4 \tag{4}$$

$$a_s=\frac{0.321-1.3R_2}{0.35L_x^2},\quad b_s=\frac{2(0.964+0.24R_2)}{L_x},\quad c_s=-0.27 \tag{5}$$

Here t_s is the time required for the heat flux distribution to reach the steady-state profile. The value of t_s is calculated as follows [14]:

$$\begin{aligned} \hat{t}&=11.7\exp(-0.123\hat{V}) \quad \hat{V}\geqslant 20 \\ \hat{t}&=1.3\exp(-0.0164\hat{V}) \quad \hat{V}\leqslant 20 \end{aligned} \tag{6}$$

Here

$$\hat{t}=\frac{\alpha_T t_s}{d^2},\quad \hat{V}=\frac{Vd}{\alpha_T}$$

Where V is the cutting speed, d is the depth of cut and α_T is the thermal diffusivity of the cutting tool.

In the analysis to be presented, the heat flux variation with time is assumed to be known (see Eq. (2)). The contact area can be determined from experimental measurements, such as in Stephenson et al. [10]. First, the heat flux is determined by using the

Loewen and Shaw's model [11]. It is modified (as shown in the next section) to account for the transient energy partitioning. This model is also used to determine the approximate tool-chip interface temperature where the thermal properties are evaluated at each time step. The initial and boundary conditions are:

$$T(x,y,z,0)=T_0 \tag{7}$$

$$\left.\frac{\partial T}{\partial x}\right|_{x=d}=\left.\frac{\partial T}{\partial y}\right|_{y=0}=\left.\frac{\partial T}{\partial z}\right|_{x=f}=0 \tag{8}$$

$$T(0,y,z,t)=T(x,y,0,t)=T_0 \tag{9}$$

and either

$$T(x,e,z,t)=T_0 \tag{10}$$

for the bottom surface at the ambient temperature, or

$$\left.\frac{\partial T}{\partial y}\right|_{y=e}=0 \tag{11}$$

for an insulated bottom surface.

The solution is determined using separation of variables as in Stephenson et al. [10]. The series solution can be expressed as follows:

$$\theta(x,y,z,t)=T(x,y,z,t)-T_0$$
$$=\sum_{i=0}^{\infty}\sum_{j=0}^{\infty}\sum_{k=0}^{\infty}\Theta_{ijk}\cdot\sin\alpha_i x\cdot\cos\beta_j y\cdot\sin\gamma_k z \tag{12}$$

For the case of insulated exterior boundary conditions, the eigenvalues are:

$$\alpha_i\cdot d=\frac{2i-1}{2}\pi,\quad \gamma_k\cdot f=\frac{2k-1}{2}\pi \tag{13}$$

where γ_k depends on the choice of boundary condition:

$$\beta_j\cdot e=\frac{2j-1}{2}\pi \tag{14}$$

or bottom surface at the ambient temperature, or

$$\beta_j\cdot e=j\pi \tag{15}$$

for an insulated bottom surface.

The functions $\Theta_{ijk}(t)$ are calculated such that the governing differential equation and the initial condition are satisfied:

$$\frac{d\Theta_{ijk}}{dt}+\omega_{ijk}\Theta_{ijk}=\Omega_{ijk}(t) \tag{16}$$

and $\Theta_{ijk}(0)=0$, where

$$\omega_{ijk}=\alpha_T(\alpha_i^2+\beta_j^2+\gamma_k^2) \tag{17}$$

and

$$\Omega_{ijk}=\alpha_T\frac{Q_{ijk}(t)}{K_t I_i J_j K_k} \tag{18}$$

with I_i, J_j, K_k, are normalized constants given by:

$$I_i=\int_0^d\sin^2\alpha_i x\,dx=\frac{d}{2}-\frac{\sin 2\alpha_i d}{4\alpha_i}$$

$$K_k=\int_0^f\sin^2\gamma_k z\,dz=\frac{f}{2}-\frac{\sin 2\gamma_k f}{4\gamma_k} \tag{19}$$

$$J_j=\int_0^e\cos^2\beta_j y\,dy=\frac{1}{\beta_j}\left(\frac{e\beta_j}{2}+\frac{\sin 2\beta_j e}{4}\right)$$

It can be seen from the equations that if the exterior boundaries are insulated, then the third equation can be simplified to:

$$J_j=\frac{e}{2}+\frac{\sin 2\beta_j e}{4\beta_j} \tag{20}$$

The forcing term in the ordinary differential equation is obtained from:

$$Q_{ijk}(t)=\int_0^d\int_0^e\int_0^f q(x,y,z,t)\sin\alpha_i x\cdot\cos\beta_j y\cdot\sin\gamma_k z\,dz\,dx\,dy$$
$$=q_c^*(\alpha(t)\cdot in_2+b(t)\cdot in_1+c(t)\cdot in) \tag{21}$$

Where in_2, in_1, and in can be expressed as follows:

$$in_2=\left[\frac{(d-L_x)^2}{\alpha_i}\cos\alpha_i(d-L_x)-\frac{d^2}{\alpha_i}\cos\alpha_i d\right]$$
$$+\left[\frac{2d}{\alpha_i}\sin\alpha_i d-\frac{2(d-L_x)}{\alpha_i^2}\sin\alpha_i(d-L_x)\right]$$
$$+\frac{2}{\alpha_i^3}(\cos\alpha_i d-\cos\alpha_i(d-L_x)) \tag{22}$$

$$in_1=\frac{(d-L_x)}{\alpha_i}\cos\alpha_i(d-L_x)-\frac{d^2}{\alpha_i}\cos\alpha_i d$$
$$+\frac{1}{\alpha_i^2}(\sin\alpha_i d-\sin\alpha_i(d-L_x)) \tag{23}$$

$$in=\frac{1}{\alpha_i}(\cos\alpha_i(d-L_x)-\cos\alpha_i d) \tag{24}$$

A similar approach as in Stephenson et al. [10] is adopted to find the analytical solution based on the concept of expressing heat flux as piecewise constant, i.e., $q_c''(t)\approx q_p$ for $\tau_{p-1}<t<\tau_p$. Then the solution (where the subscript p on any quantity implies its value in the time period $\tau_{p-1}<t<\tau_p$):

$$\Theta_{ijk,1}=-\frac{\Omega_{ijk,1}}{\omega_{ijk}}[e^{-\omega_{ijk}t}-1]$$
$$\Theta_{ijk,p}=\left[\Theta_{ijk,p-1}(\tau_{p-1})-\frac{\Omega_{ijk,p}}{\omega_{ijk}}\right]\cdot e^{-\infty_{ijk}(t-\tau_{p-1})}+\frac{\Omega_{ijk,p}}{\omega_{ijk}} \tag{25}$$

Where $p=2,3,\ldots$ in the above equation.

Once the solution is determined, the average tool-chip interface temperature can be found by integrating the temperature analytically over the heat source area:

$$\theta_{ave}(t)=\frac{1}{L_x L_z}\int_{d-L_x}^{d}\int_{f-L_z}^{f}\theta(x,0,z,t)\,dx\,dz$$
$$=\frac{1}{L_x L_z}\sum_{i=1}^{\infty}\sum_{j=1}^{\infty}\sum_{k=1}^{\infty}\Theta_{ijk}(t)$$
$$\times\frac{\cos\alpha_i(d-L_x)-\cos\alpha_i d}{\alpha_i}\,\frac{\cos\gamma_k(f\text{-}L_z)-\cos\gamma_k f}{\gamma_k} \tag{26}$$

Detailed series convergence tests have been performed in this study for typical cases by comparing solutions of Eq. (26) for $100\times100\times100$ terms and for $120\times120\times120$ terms. It was found that the difference between two solutions was less than 2 percent in the initial transient, and less than 0.5 percent at larger time. Thus, $100\times100\times100$ terms is considered sufficient and is used throughout this study.

Loewen and Shaw's Model. Loewen and Shaw [11] is one of the most cited papers in the analytical study of cutting temperature prediction (e.g., [14,15,16]). A historical review on this method can be found in Komanduri [18]. A brief introductory

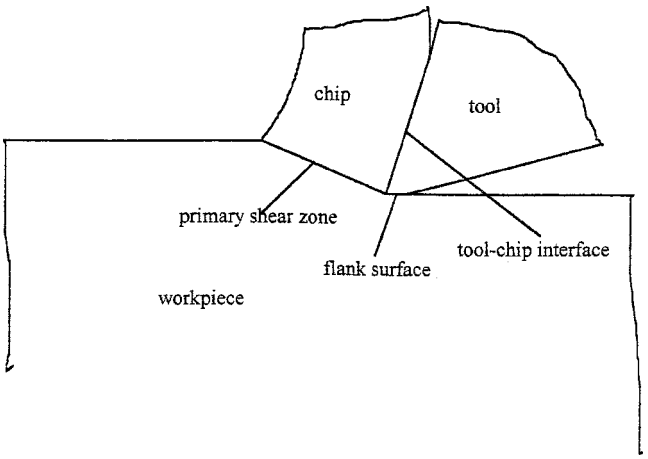

Fig. 2 Heat generation locations

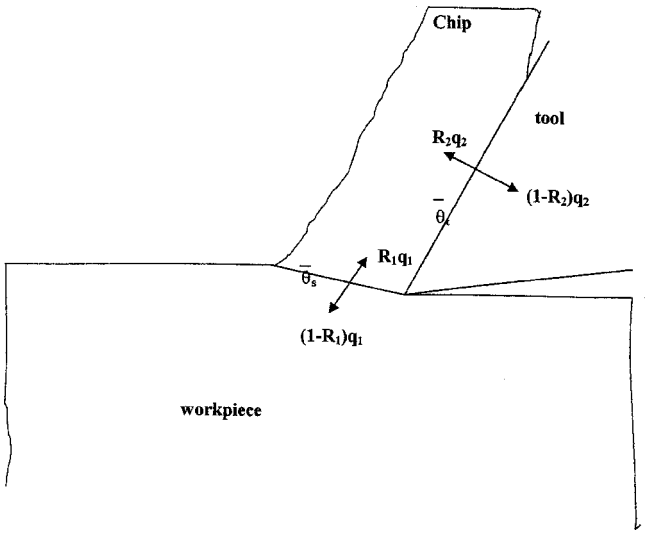

Fig. 3 Energy partitioning diagram

review will be presented, followed by the modification that has been made to account for the transient effect in the model.

In any cutting processes, almost all the mechanical work is transformed into heat. Heat is generated at three locations: the tool-chip interface, the tool flank face and the primary shear zone. A schematic diagram of these locations is shown in Fig. 2. Heat is generated at the first two locations due to frictional forces, and at the third due to plastic deformation. In their model, the heat generated at the tool flank face is assumed to be negligible. The following assumptions are imposed in Loewen and Shaw's model [11]:

1 All the energy expended at shear zone and tool-chip interface is converted to thermal energy.
2 The energy at tool-chip interface and shear zone is concentrated on a plane surface.
3 The energy at tool-chip interface and shear zone is uniformly distributed.

With the above assumptions and Jaeger's moving heat source theory [19], the temperature distributions at the tool-chip interface and the shear zone can be calculated analytically provided the energy into each component is known *a priori*. Finally, in order to determine the energy fraction into each material, Blok's [20] energy partitioning method was used to estimate the energy partitioning into each of the materials. For simplicity, this was done by matching the average temperature at the primary shear zone and at the tool-chip interface. The energy partitioning diagram is illustrated in Fig. 3.

Shear Plane Temperature. In the primary shear plane, the situation is modeled as a friction slider so Jaeger's moving heat sources theory can be applied directly. If R_1q_1 is the heat per unit area which leaves the shear zone with the chip, then $(1-R_1)q_1$ is the heat per unit time per unit area that flows into the workpiece, as shown in Fig. 3. The average temperature of the chip in the vicinity of the shear plane, and at the workpiece in the vicinity of the primary shear zone can be expressed as follows:

Chip:

$$\bar{\theta}_s = R_1 q_1 f_{1c} + \theta_0 \tag{27}$$

Workpiece:

$$\bar{\theta}_s = (1-R_1) q_1 f_{1w} + \theta_0 \tag{28}$$

The average temperatures at the shear plane must be equal, so we can equate the above two equations. It follows that:

$$R_1 = \frac{1}{1+\dfrac{f_{1c}}{f_{1w}}} \tag{29}$$

Where f_{1c} and f_{1w} are all known quantities (see Shaw [3] for details).

Tool-Chip Interface. Similarly to the primary shear zone, the moving heat sources solution is applied to the chip. For the tool temperature at the tool-chip interface, a three-dimensional steady-state conduction equation was solved using a Green's function approach. It is worth noting that both solutions are for a semi-infinite body. The average temperatures at the chip and at the tool in the vicinity of the tool-chip interface are:

Chip:

$$\bar{\theta}_t = R_2 q_2 f_{2c} + \bar{\theta}_s \tag{30}$$

Tool:

$$\bar{\theta}_t = (1-R_2) q_2 f_{2t} + \theta_0 \tag{31}$$

Again, the average temperatures at the shear plane must be equal. Thus, we can equate the above two equations to get:

$$R_2 = \frac{1+\dfrac{\theta_0 - \bar{\theta}_s}{q_2 f_{2t}}}{1+\dfrac{f_{2c}}{f_{2t}}} \tag{32}$$

Where f_{2c} and f_{2t} are known quantities (see, Shaw [3] for detail).

In Loewen and Shaw's model, time is assumed to approach infinity, i.e., the quasi-steady condition. Thus, in principle, their results are valid only when the cutting action (i.e., heating) is under steady-state conditions. As mentioned earlier, a steady-state temperature solution may not be achieved in real industrial machining processes due to the fact that the depth of cut, cutting speed and feed rate may all vary with time. In the works by Stephenson and Ali [8] and Stephenson et al. [10], they showed that Loewen and Shaw's model gave reasonable temperature predictions when the cutting acting is continuous or is long enough so that the temperature distribution is essentially quasi-steady (although the parameters are all varying with time). However, when the cutting time (i.e., heating time) relative to the uncut time (i.e., cooling time) is short, as in milling operations, the predicted temperature using Loewen and Shaw's model tends to be significantly lower than the actual temperature measured [8].

In this study, we propose a simple approximation to evaluate the energy partition under transient conditions. Note that the solutions that we have for the tool are exact solutions to the three-dimensional transient energy equation. Thus, the tool-chip interface temperature at the tool side represents the exact solution. Second, we further assume that the quasi-steady solution from Loewen and Shaw's model is still valid for the primary shear zone, and the tool-chip interface temperature at the chip side. These assumptions can be justified by considering the simplified model of a rectangular heat source moving on a horizontal surface. By integrating from a point moving heat source to the rectangular moving heat source [12], it can be found that the time to reach steady state is less than 10^{-3} seconds under typical cutting conditions. This indicates that almost immediately after the cutting action begins, the temperature at the heat source reaches the steady state condition. Based on the above assumptions, it can be seen that the only unknown in evaluating the energy partition that enters the chip through the tool-chip interface (R_2) is f_{2t}. This can be modeled by the following iterative procedure.

From the equation at chip side, Eq. (30), after rearranging:

$$R_2 = \frac{\overline{\theta} - \overline{\theta}_s}{q_2 f_{2c}} \tag{33}$$

(a) Guess ${R_2}^{n+1}$
(b) Calculate θ_t
(c) Update ${R_2}^{n+2}$ from the above equation
(d) Repeat (b)–(c) until it converges.

Note that the thermal properties of the tool and workpiece are updated in each iteration based on the calculated tool-chip interface temperature. The temperature dependent thermal properties are evaluated using the 2nd order polynomial listed in Stephenson [6]. With the above-calculated transient energy partition, the average tool temperature distribution can be evaluated directly. By imposing the empirically estimated heat flux distribution, the tool-chip interfacial local temperature distribution can be calculated. The transient average tool-chip temperature predicted by the analysis is compared with experimental data, and the effect of transient energy partitioning in comparison to the Loewen and Shaw's model will be shown. The effect of nonuniform heat flux distribution on the temperature distribution will also be demonstrated.

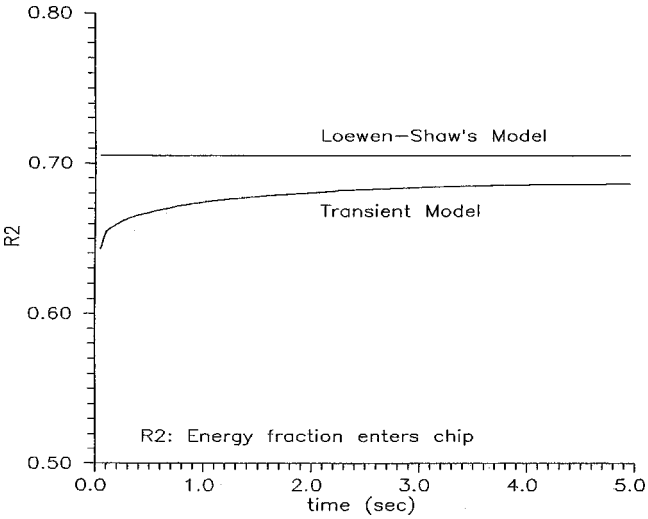

Fig. 4 Comparison of transient and steady state energy partitioning

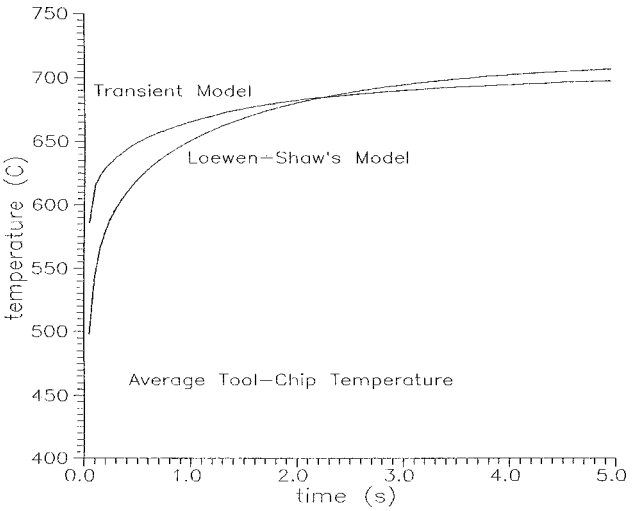

Fig. 5 Comparison of tool temperature distributions in transient and steady state model

Results and Discussions

Transient Energy Partitioning. The transient tool energy partitioning was calculated for the same conditions as in Stephenson et al. [10]. In the case depicted in Fig. 4, the tool is made of *C*2 grade uncoated tungsten carbide, with side rake, back rake, and lead angles of −5°, 0°, and 10°, respectively. The final tool dimensions were $d=8.3$ mm, $e=2.65$ mm, and $f=102$ mm. The cutting speed, feed rate and depth of cut are 61.5 m/min, 0.127 mm/rev, and 0.381 mm, respectively. The material being cut is cold drawn 1018 steel. More detailed information can be found in Stephenson et al. [10]. Unless otherwise stated, all the cases demonstrated in the following sections use the tool and cutting specifications listed above. The transient energy partitioning calculated from the present analysis is compared to the quasi-steady energy partitioning obtained from the Loewen and Shaw model (see Fig. 4). It can be seen from the figure that the energy partition R_2, which corresponds to the energy that enters the chip, is smaller for small time. For increasing time, the energy partition R_2 calculated by the transient model approaches that computed by Loewen and Shaw's model. This means that there is more energy entering the tool in the early transient period, a reasonable result since the tool is cooler at the very beginning of the cut. The corresponding average tool temperature at the tool-chip interface is demonstrated in Fig. 5. The transient model predicts higher temperature in the early transient period, with the temperature approaching that predicted by Loewen and Shaw's model as time increments.

Comparison to Experimental Data. To verify the model predictions, cutting conditions as in Stephenson and Ali [8] were computed with the present model. Stephenson and Ali had reported both computed and measured average tool-chip interface temperatures during end turning on a slotted tube workpiece. The cutting process was designed such that four cutting and four non-cutting periods occur during one workpiece revolution. The tool-chip interface temperature was measured using a tool-workpiece thermocouple method. Model calculations were made for all cases as in Stephenson and Ali [8]. Agreement with the published experimental results was seen to be good. One representative case is discussed in detail here. The case in point is the one where 2024 aluminum was used, with $\tau_1=0.0184$s and $\tau_2=0.0249$s (where τ_1 is the cutting (heating) time, and τ_2 is the uncut (cooling) time). The tool insert geometry was $d=f=8.255$ mm and $e=2.54$ mm. The results are shown in Fig. 6. For the purposes of comparison, the results from the previous model [10] and Radulescu and Kapoor [9] are also depicted in the figure. It is seen that the interior boundary conditions at $y=e$ (i.e., insulated or isothermal)

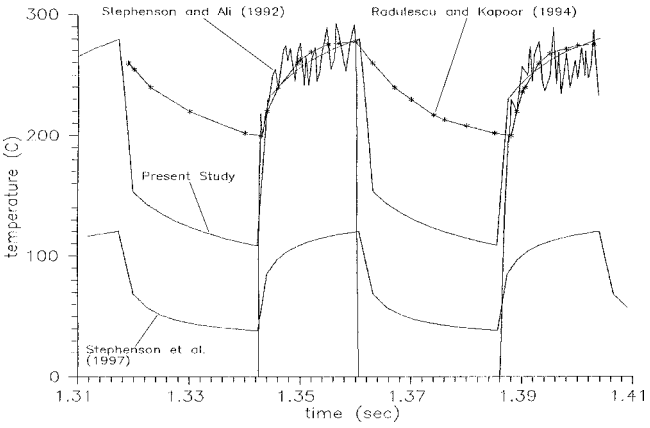

Fig. 6 Comparison of experimental data with predicted temperatures

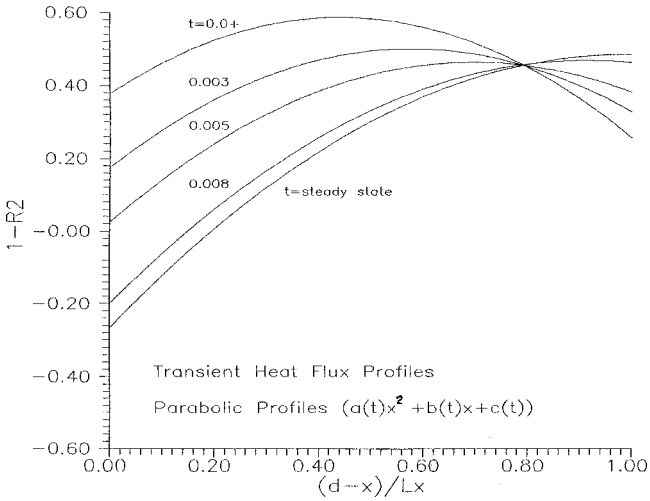

Fig. 7 Transient heat flux profiles

do not affect the solution. This is reasonable because the penetration depth is not large enough to reach the interior boundary at $y=e$ due to the very short heating and long cooling cycle. The broken lines in the experimental data are due to the initial transient emf signal responses (i.e., cut-ins). Note that the measured temperatures that went to zero at the initial cut-in are clearly spurious. Figure 6 indicates that the model predictions agree quite well with experimental data. It is worth noting that there is a very sharp increase in the tool temperature at the initial transient period at every cut-in. The present transient analysis also gives a very accurate prediction in this early transient period. The temperatures predicted using Radulescu and Kapoor's model [9] agree well with the experimental data except for the local minimum temperatures. It appears that the present model performs better in this aspect because of the fact that the present model uses variable thermal properties locally while their model assumes constant thermal properties.

Nonuniform Heat Flux Distribution. It has been shown experimentally that the maximum temperature at the tool-chip interface is somewhere in the middle of the tool-chip contact surface (e.g., [21]). The importance of the location of the maximum temperature is its direct relation to crater wear [15,21]. In most of the analytical work on predicting local tool-chip temperature distributions, a uniform heat flux was assumed (e.g., [8,9,10,11]) at the tool-chip interface. This is a natural choice because Loewen and Shaw's model assumed uniform heat flux at both the primary shear zone and the tool-chip interface. However, as indicated by Chao and Trigger [15], the local tool-chip interface temperature distribution *does not* match for the chip side temperature and the tool side temperature because Loewen and Shaw's model only requires the matching of the average tool-chip interface temperature. The consequence of assuming uniform heat flux is that the maximum tool temperature is located at the cutting tip instead of somewhere in the middle of the tool-chip contact area. Chao and Trigger [15] tried to correct this deficiency by calculating the tool-chip temperature distribution at the chip side using Jaeger's moving heat source theory [19], and matching the temperature semiempirically to the tool-chip interface temperature at the tool side. From this temperature matching, they obtained a local energy partitioning. Time consuming iteration is required for this procedure. As an alternative, we developed the local energy partitioning by curve fitting the data obtained from the work presented by Levy et al. [16]. A parabolic profile is assumed to approximate the local heat flux distribution at the tool side. Here, the transient average energy partitioning is obtained from the transient energy partitioning analysis presented in the earlier section.

Previous published studies [14,16] showed that the heat flux profile varies with time during the initial transient. In order to account for this behavior, we use the transient model proposed by Kagiwada and Kanauchi [14] to predict the time required to reach the steady-state profile. The transient heat flux profiles are shown in Fig. 7. It can be seen that the $(1-R_2)$ (i.e., energy partitioning entering the tool) value is greater than zero in the early transient period. As the profiles approach the steady state profile, the value of $(1-R_2)$ near the tool tip at the tool-chip interface gradually becomes less than zero. This behavior can be explained as follows. When the tool first cuts into the material, the tool is cooler than the chip, resulting in a positive contribution to the energy partition. As time progresses, the tool becomes hotter, particularly at the tool tip, due to the inefficient dissipation of heat. Eventually, a point is reached where the energy partitioning becomes negative near the tool tip area. The analytical steady-state results from Chao and Trigger [15] confirmed this trend.

The local transient temperature distribution at the tool-chip interface is plotted in Fig. 8. It can be seen that early in the transient state (i.e., the curve for $t=0.003$s), the maximum temperature is located very close to the cutting tip of the tool insert. This simply reflects the fact that in the initial transient, the energy partitioning is positive. Thus, the maximum temperature is pushed to the cutting tip due to the insulated boundary condition imposed at the

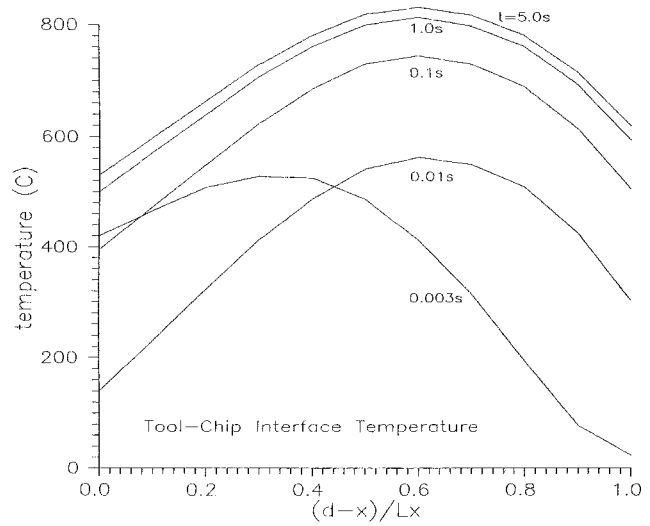

Fig. 8 Transient tool-chip interface temperature distributions

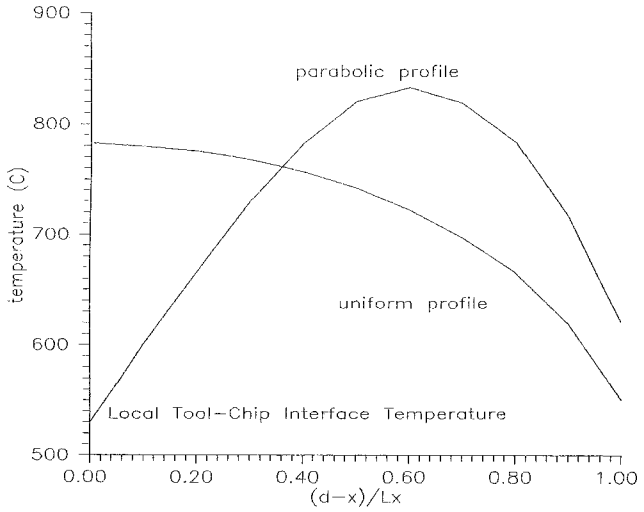

Fig. 9 Comparison of local tool-chip interface temperatures for uniform and parabolic heat flux inputs

exterior boundaries. As time progresses, the heat flux profile becomes steady. A sequence of temperature profiles shows that the profiles remain essentially the same, with the magnitude increasing with time. It is observed that the location of maximum temperature moves rapidly towards the center of the tool-chip contact area. This is because the heat flux profiles change quickly from transient to steady state due to short transient time for heat flux profile. Note that the decrease in the tool-chip interface temperature near the cutting tip at the transient state is due to the decrease in the energy partitioning at the cutting tip (see Fig. 7 for details).

A comparison of local temperature distribution at the tool-chip interface for the uniform and parabolic heat flux inputs is presented in Fig. 9. The local temperature distributions under steady state condition are plotted along the tool-chip contact length. For the case of uniform heat flux input, the maximum temperature is located, as expected, at the cutting tip of the tool. With the proposed parabolic profile, the maximum temperature moves toward the center of the tool-chip contact area, at $(d-x)/L_x \approx 0.65$ for the case shown in Fig. 9. This agrees qualitatively with the experimental data shown in Trent [21].

Summary and Conclusion

This paper describes an improved model for calculating tool temperatures under initial transient and cut-in conditions, with time varying heat flux and tool-chip contact area. The model is based on an analytical solution for the temperature in a rectangular insert subjected to a variable heat flux distribution. The Loewen and Shaw model is modified to account for the effect of the initial transient, and the transient energy partitioning calculated. It has been shown that the energy partitioning is larger in the initial transient state. Calculated temperatures based on this transient energy partitioning agree very well with experimental data. A semi-empirical parabolic heat flux profile is proposed in this study. The calculated local temperature distribution agrees qualitatively with experimental evidence. The simulated maximum temperature is located somewhere in the center of the tool-chip contact area. This fact could be important in determining crater tool wear.

The utility of such a transient cutting model is twofold. First, a model that predicts the transient tool temperatures can be used to optimize the cutting processes to reduce the tool wear at the tool-chip interface. Second, a predictive model can be used for adaptive control of the cutting process. During cutting, the cutting power can be easily monitored. If the measured cutting power, when used as an input to the predictive model, indicates the tool temperature is approaching a level that may accelerate the tool wear, then the cutting parameters can be automatically adjusted to reduce the tool temperature.

Acknowledgments

Dr. Tien-Chien Jen would like to thank General Motors and the Society of Manufacturing Engineers (Research Initiation Award) for their financial support of the project. The authors are grateful to Dr. David Stephenson and Dr. Pulak Bandyopadhyay for their helpful discussion of the results. Acknowledgment also is made to Dr. Stanley Chen for his assistance in proofreading.

Nomenclature

$a(t)$ = leading coefficient of the parabolic profile, Eq. (3)
a_0 = coefficient $a(t)$ at zero time
a_s = coefficient $a(t)$ at steady state
$b(t)$ = second coefficient of the parabolic profile, Eq. (3)
b_0 = coefficient $b(t)$ at zero time
b_s = coefficient $b(t)$ at steady state
$c(t)$ = Third coefficient of the parabolic profile, Eq. (3)
c_0 = coefficient $c(t)$ at zero time
c_s = coefficient $c(t)$ at steady state
d = tool insert dimension in the x direction
e = tool insert dimension in the y direction
f = tool insert dimension in the z direction
f_{1c}, f_{1w} = shear plane model parameters
f_{2c}, f_{2w} = tool-chip contact surface parameters
i,j,k = dummy index
k_T = tool thermal conductivity
I_i, J_j, K_k = integrals in Eq. (19)
in, in_1, in_2 = integrals in Eqs. (22)–(24)
L_x = tool-chip contact length in x direction
L_z = tool-chip contact length in z direction
p = dummy index
Q_{ijk} = forcing term in Eq. (21)
$q(x,y,z,t)$ = heat source term, Eq. (1)
$q_c''(t)$ = average heat flux in each time step
q_p = average heat flux at each time step
q_1, q_2 = total heat flux at primary shear zone and tool-chip interface
R_1, R_2 = energy partition into the chip from the primary shear zone and tool-chip interface
t = time
T = temperature
V = velocity
x,y,z = Cartesian coordinate

Greek Symbols

α = thermal diffusivity
$\alpha_i, \beta_j, \gamma_k$ = eigenvalues
τ = time interval
θ = temperature rise relative to the ambient temperature
ω_{ijk} = coefficient of the ordinary differential equation, Eq. (17)
Θ_{ijk} = function of the differential equation, Eq. (16)
Ω_{ijk} = coefficient of the differential equation, Eq. (18)

Subscripts and Superscripts

av = average value
0 = initial or ambient quantities
s = steady state condition
T,t = tool
$\wedge$ = dimensionless parameters
$-$ (overbar) = average quantity

References

[1] Trigger, K. J., and Chao, B. T., 1951, ''An Analytical Evaluation of Metal Cutting Temperatures,'' Trans. ASME, **73**, pp. 57–68.

[2] Barrow, G., 1973, ''A Review of Experimental and Theoretical Techniques for Assessing Cutting Temperatures,'' CIRP Ann., **22**, pp. 203–211.

[3] Shaw, M. C., 1984, *Metal Cutting Principles*, Oxford University Press, Oxford, Chap. 12.

[4] Boothroyd, G., and Knight, W. A., 1989, *Fundamentals of Machining and Machine Tools*, Marcel and Dekker, New York, Chap. 3.

[5] Strenkowski, J. S., and Moon, K. J., 1990, ''Finite Element Prediction of Chip Geometry and Tool/Workpiece Temperature Distribution in Orthogonal Machining,'' ASME J. Eng. Ind., **112**, pp. 313–318.

[6] Stephenson, D. A., 1991, ''Assessment of Steady-State Metal Cutting Temperature Models Based on Simultaneous Infrared and Thermocouple Data,'' ASME J. Eng. Ind., **113**, pp. 121–128.

[7] Chandra, A., and Chen, C. L., 1994, ''Thermal Aspects of Machining: A BEM Approach,'' Int. J. Solids Struct., **33**, pp. 1657–1693.

[8] Stephenson, D. A., and Ali, A., 1992, ''Tool Temperature in Interrupted Cutting,'' ASME J. Eng. Ind., **114**, pp. 127–136.

[9] Radulescu, R., and Kapoor, S. G., 1994, ''An Analytical Model for Prediction of Tool Temperature Fields during Continuous and Interrupted Cutting,'' ASME J. Eng. Ind., **116**, pp. 135–143.

[10] Stephenson, D. A., Jen, T. C., and Lavine, A. S., 1997, ''Cutting Tool Temperatures in Contour Turning: Transient Analysis and Experimental Verification,'' ASME J. Manuf. Sci. Eng., **119**, pp. 494–501.

[11] Loewen, E. G., and Shaw, M. C., 1954, ''On the Analysis of Cutting Tool Temperatures,'' Trans. ASME, **76**, pp. 217–231.

[12] Carslaw, H. S., and Jaeger, J. C., 1959, *Conduction of Heat in Solids*, Clarendon Press, Oxford.

[13] Jen, T. C., and Lavine, A. S., 1994, ''Prediction of Tool Temperatures in Interrupted Metal Cutting,'' *Proc. of 7th International Symposium on Transport Phenomena in Manufacturing Processes*, pp. 211–216.

[14] Kagiwada, T., and Kanauchi, T., 1988, ''Numerical Analyses of Cutting Temperatures and Flow Ratios of Generated Heat,'' JSME Int. J., Ser. III, **31**, No. 3, pp. 624–633.

[15] Chao, B. T., and Trigger, K. J., 1955, ''Temperature Distribution at the Tool-Chip Interface in Metal Cutting,'' Trans. ASME, **77**, pp. 1107–1121.

[16] Levy, E. K., Tsai, C. L., and Groover, M. P., 1976, ''Analytical Investigation of the Effect of Tool Wear on the Temperature Variations in a Metal cutting Tool,'' ASME J. Eng. Ind., **98**, pp. 251–257.

[17] Tsai, C. L., 1973, *Finite Difference Solutions for the Time Dependent Temperature Distributions in Metal Cutting Tool*, MS thesis, Department of Mechanical Engineering and Mechanics, Lehigh University.

[18] Komanduri, R., 1993, ''Machining and Grinding: A Historical Review of the Classical Papers,'' Appl. Mech. Rev., **46**, No. 3, pp. 80–132.

[19] Jaeger, J. C., 1942, ''Moving Sources of Heat and the Temperature at Sliding Contacts,'' Proc. Roy. Soc. NSW, **76**, pp. 203–224.

[20] Blok, H., 1938, ''Theoretical Study of Temperature Rise at Surfaces of Actual Contact Under Oiliness Lubricating Conditions,'' *Proc. General Discussion on Lubrication and Lubricants, Inst. Mech. Eng.* (London), pp. 222–235.

[21] Trent, E. M., 1977, *Metal Cutting*, Butterworth, Washington, DC, Chap. 5.